Thermal Entanglement of superconducting qubits for arbitrary interaction strength

Areeda Ayoub[1] and Javed Akram[1,∗]

[1]*Department of Physics, COMSATS University Islamabad, 44000, Islamabad Pakistan*

(Dated: November 2, 2022)

We investigate the thermal entanglement in two superconducting qubits for arbitrary interaction strength and ground state frequencies. We calculate the concurrence of the system to quantify the thermal entanglement. We suggest a scheme, where an external tunable coupler qubit sandwich between two superconducting qubits generates entanglement. The behavior of concurrence is analyzed for three different cases, in which we consider the effects of the temperature, the qubit-qubit effective coupling strength, and the qubit frequencies on the thermal entanglement. What deserves mentioning here is that to achieve maximally entangled states, it is better to use two superconducting qubits with the same frequencies. We also note that for a given temperature, the thermal entanglement can be tuned by qubit internal capacitance and inductance.

I. INTRODUCTION

From the first idea of a quantum computer by Feynman in 1982, the race for the transition from classical computers to the quantum computer has been going on. The key to achieve this is by replacing the classical bit with the superconducting qubit. Superconducting qubits have attracted the attention of scientists not only for their high speed and efficiency but the versatile nature of their quantum states that can be engineered and controlled [1–4]. A physical system that is required to process quantum information must obey quantum mechanical laws like superposition and entanglement. The states of the composite system are entangled when they cannot be defined in the form of the product of states of the individual system. The simplest composite system that can exhibit entanglement consists of two-level systems (with ground $|0\rangle$ and excited $|1\rangle$ states). To perform quantum information processing, superconducting qubits are the most suitable candidates. Therefore, the generation of superconducting qubits and processing of information with these qubits are the main questions that need to be investigated. Additionally, it is also equally important to explore environmental noises and temperature effects on the superconducting qubits [5–9]. The coherence of superconducting qubits is greatly improved by reducing their sensitivity to the charge noise via shunting a large capacitance to the Josephson junction. This was first proposed for capacitively shunted flux qubit in [10] and later experimentally realized in [11, 12]. Later it was also proposed for the Transmon qubits in [13] and implemented in [14]. Nowadays, the main focus of scientific research is to preserve these states from decoherence by taking advantage of effective coupling, which can be constructed between the superconducting qubits by interaction with a common tunable coupler [15].

From the last few years, entanglement has been thoroughly investigated [16, 17]. Entanglement has non-classical nature, therefore it helps to study conceptual foundations of quantum mechanics. Interpretation of quantum information processing is not possible without an understanding of quantum entanglement, and interaction of entanglement with the environment becomes very sensitive to do quantum computing and quantum information processing. Experimentalists always want to preserve entanglement for a longer period. However, in the real world, it is quite tough to protect the system from the environment, especially from the thermal environment. Therefore, in this paper, we investigate the effect of temperature on the entanglement, which we generated by using two coupled superconducting qubits [18–20]. Additionally, we also study the effect of interaction strength and ground state frequencies on the thermal entanglement.

In this work, we introduce the simple and widely applicable method of using a tunable coupler to couple two superconducting qubits to generate entanglement. It consists of generic three-body systems with exchange-type interaction. The coupler is a central component that not only helps to exchange interaction between two qubits but also helps to tune the coupling strength between the next-nearest neighbor [21].

For a quantum mechanical system in thermal equilibrium at temperature T, the density matrix can be composed as $\rho = e^{-\beta H}/Z$, where, H describes the Hamiltonian of the system, $Z = tre^{-\beta H}$ defines the partition function and $\beta = 1/(k_B T)$ where k_B illustrate the Boltzman constant. The thermal entanglement of two qubit system can be determined by the concurrence C_E which is given by the *Wootter's* formula [22] as $C_E = max[0, 2\,max[\lambda_i] - \sum_{i=1}^{4} \lambda_i]$. Here λ_i is the square root of the eigen values of the matrix $R = \rho(\sigma_1^y \otimes \sigma_2^y)\rho^*(\sigma_1^y \otimes \sigma_2^y)$, where $*$ represents the complex conjugate. The concurrence C_E can be defined for both mixed and pure states, ranges from 0 to 1. In general, we can define the two qubit composite system state as

$$|\phi\rangle = a\,|00\rangle + b\,|01\rangle + c\,|10\rangle + d\,|11\rangle, \qquad (1)$$

here, $|\phi\rangle \in H_A \otimes H_B$, the two systems are separable if and only if $ad = bc$. Therefore, we can define concur-
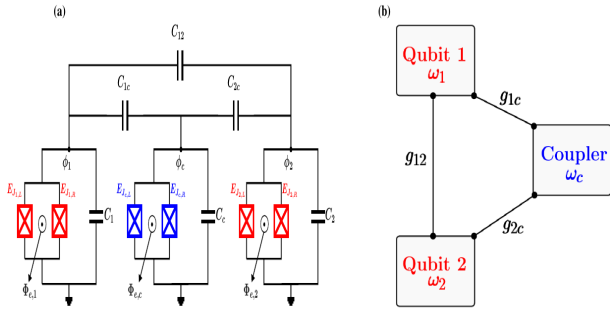
FIG. 1: Schematic diagram of implementing superconducting qubits, consisting of qubit modes $(1, 2)$ and coupler mode c. Here, C_λ is the dominant mode capacitance, C_{jc} describes the coupling capacitance between qubit j and coupler, C_{12} illustrates the direct coupling capacitance between the qubits and ϕ_λ represents the reduced node flux. Here, $E_{J_{\lambda, L(R)}}$ is the defined as a Josephson energy of the left (right) junction mode $\lambda = (1, 2, c)$. In Fig. (b) we plot a block diagram of two qubits coupled with tunable coupler ω_c, where qubit have frequencies ω_1 and ω_2

rence as $C_E(\psi) = 2|ad - bc|$. In this respect, we organize this paper as follows. We discuss the modeling of the qubit and coupled qubits in Sec. II. We introduce a method in Sec. III, through which interaction between the superconducting qubits can be engineered to implement two coupled qubit entangling operations. We also discuss how temperature, effective qubit-qubit coupling strength, and qubit frequencies affect thermal entanglement. The conclusion is given in Sec. IV.

II. THEORETICAL MODEL

A. Modeling of a Qubit

A superconducting circuit needs some non-linear element to function as a qubit and this non-linearity is provided by the Josephson Junction, which forms the backbone of superconducting circuits. Josephson junction is based on two superconductors separated by a very thin layer of an insulator to allow tunneling of discrete charges across the junction [23], the superconducting qubit circuit consists of a capacitor and Josephson junction as shown in Fig. 1(a). The energy of the circuit elements is defined as

$$E(t) = \int_{-\infty}^{t} V(t')I(t')dt'. \tag{2}$$

where $V(t')$ and $I(t')$ represent the voltage and current of the capacitor or non-linear inductor. According to Faraday's law, flux can be defined as $\Phi(t) = \int_{-\infty}^{t} V(t')dt'$. By using relation for the current flowing through the capacitor $I = C\frac{dV}{dt}$, we derive the kinetic energy stored in the capacitor with capacitance C in terms of node flux as

$T = \frac{1}{2}\left(\frac{\hbar}{2e}\right)^2 C\dot{\phi}^2$, where $\phi = 2\pi\Phi/\Phi_0$ is the reduced flux and $\Phi_0 = h/2e$ is the superconducting magnetic flux. The potential energy of the Josephson junction can be derived by using Eq. (2) as $U = E_J(1 - \cos\Phi)$, where $E_J = \hbar I_c/2e$ is the Josephson energy which depends on the barrier transparency and superconducting gap [24]. The Hamiltonian of the single qubit can be written as

$$\hat{H} = 4E_C\hat{n}^2 - E_J(1 - \cos\hat{\phi}), \tag{3}$$

where $\hat{n} = q/2e$ is the number of Cooper pairs and $E_C = e^2/2C$ defines the charging energy of the capacitor. Since $\hat{\phi}$ is very small, by expanding the potential term of the Eq. (3) into power series, we get approximate Hamiltonian as

$$\hat{H} = 4E_C\hat{n}^2 + \frac{1}{2!}E_J\hat{\phi}^2 - \frac{1}{4!}E_J\hat{\phi}^4. \tag{4}$$

By introducing the creation $(\hat{b}^\dagger)$ and annihilation $(\hat{b})$ above Hamiltonian can be rewritten as

$$H = \sqrt{8E_JE_C}\left(\hat{b}^\dagger\hat{b} + \frac{1}{2}\right) - \frac{E_C}{12}|\hat{b}^\dagger + \hat{b}|^4, \tag{5}$$

where $\hat{n}$ and $\hat{\phi}$ are defined as $\frac{i}{2}\sqrt[4]{\frac{E_J}{2E_C}}(\hat{b}^\dagger - \hat{b})$ and $\sqrt[4]{\frac{2E_C}{E_J}}(\hat{b}^\dagger + \hat{b})$, respectively. Here, annihilation and creation operators follow commutation relation as $[\hat{b}, \hat{b}^\dagger] = 1$. Neglecting the constant term and fast-oscillating terms, the Hamiltonian of the system resembles the Duffing oscillator $(\hbar = 1)$, which is a harmonic oscillator plus an additional quartic term

$$H = \omega\hat{b}^\dagger\hat{b} + \frac{\alpha}{2}\hat{b}^\dagger\hat{b}^\dagger\hat{b}\hat{b}. \tag{6}$$

where $\omega = \sqrt{8E_JE_C} - E_C$ defines the transition frequency and $\alpha = -E_C$ describes the anharmonicity in the system. If the anharmonicity is sufficiently large then excitation to higher states is suppressed and the lowest two levels can be treated as a two-level qubit system. And the quantum two-level simplified Hamiltonian can be represented as

$$H = \omega\frac{\sigma_z}{2}, \tag{7}$$

where σ_z is the Pauli z-operator. It is necessary to keep in mind that higher states exist, however, their influence on the system dynamics is quite small.

B. Modeling of Coupled Qubits

In this subsection, we discuss the coupling of superconducting qubits with a tunable coupler, as shown in Fig. 1(a). Each qubit is treated as a weakly anharmonic oscillator consisting of capacitor C_λ and Josephson junction, where the subscript defines as $\lambda = \{1, 2, c\}$. For
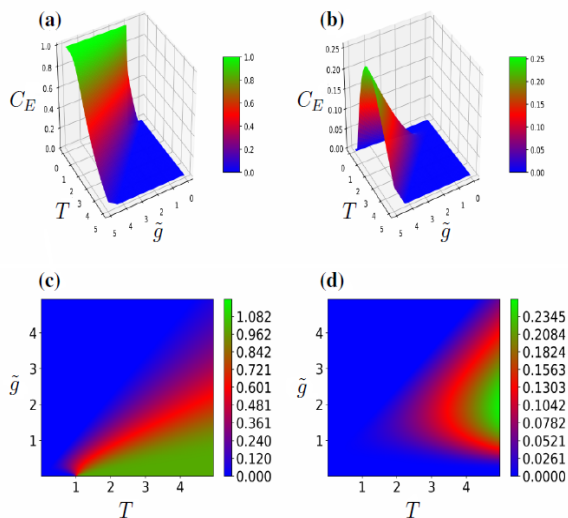
FIG. 2: The two-dimensional concurrence is plotted versus temperature T and qubit-qubit effective coupling strength $\tilde{g}$ for two coupled superconducting qubits. The left panel corresponds to $\tilde{\omega}_1 = \tilde{\omega}_2 = 1$ case and right panel corresponds to $\tilde{\omega}_1 = 5$ and $\tilde{\omega}_2 = 1$ case. T is plotted in units of Boltzmann's constant $k_B = 1$ and we work in units where $\tilde{g}$ and $\tilde{\omega}_j$ are dimensionless.

simplicity, the junction capacitance is merged into C_λ. The kinetic and potential energies of these coupled qubit systems are given as

$$
T = \frac{1}{2}\Big[C_1 \dot{\Phi}_1{}^2 + C_c \dot{\Phi}_c{}^2 + C_2 \dot{\Phi}_2{}^2 + C_{1c}(\dot{\Phi}_1 - \dot{\Phi}_c)^2 \\
+ C_{2c}(\dot{\Phi}_2 - \dot{\Phi}_c)^2 + C_{12}(\dot{\Phi}_1 - \dot{\Phi}_2)^2 \Big],
\tag{8}
$$

$$
U = E_{J_1}\Big[1 - \cos\big(\frac{2\pi}{\Phi_0}\Phi_1\big)\Big] + E_{J_c}\Big[1 - \cos\big(\frac{2\pi}{\Phi_0}\Phi_c\big)\Big] \\
+ E_{J_2}\Big[1 - \cos\big(\frac{2\pi}{\Phi_0}\Phi_2\big)\Big],
\tag{9}
$$

where T labels the kinetic energy and U specifies the potential energy. Here, Josephson Energy of individual qubits is defined as a combination of left and right Josephson junction individual energies,

$$
E_{J_\lambda} = E_{J_{\lambda,T}} \sqrt{\cos^2\big(\frac{\pi\Phi_{e,\lambda}}{\Phi_0}\big) + d_\lambda^2 \sin^2\big(\frac{\pi\Phi_{e,\lambda}}{\Phi_0}\big)}, \tag{10}
$$

where $\Phi_0 = h/2e$ is described as a superconducting quantum flux, here $E_{J_{\lambda,T}} = E_{J_{\lambda,L}} + E_{J_{\lambda,R}}$ is represented as a sum of the Josephson energies, and $d_\lambda = \big(E_{J_{\lambda,L}} - E_{J_{\lambda,R}}\big)/\big(E_{J_{\lambda,L}} + E_{J_{\lambda,R}}\big)$ is the junction asymmetry [13]. In compact form, the kinetic energy of the coupled two-qubit system can be defined as $T = \frac{1}{2}\dot{\vec{\Phi}}^T \mathbf{C}\dot{\vec{\Phi}}$, here $\mathbf{C}$ describes a 3×3 capacitance matrix [25],

$$
\mathbf{C} = \begin{pmatrix} C_{112} + C_{1c} & -C_{1c} & -C_{12} \\ -C_{1c} & C_{c2c} + C_{1c} & -C_{2c} \\ -C_{12} & -C_{2c} & C_{212} + C_{2c} \end{pmatrix}, \tag{11}
$$

where, $C_{112} = C_1 + C_{12}$, $C_{c2c} = C_c + C_{2c}$ and $C_{212} = C_2 + C_{12}$. The Hamiltonian of the system can be depicted as

$$
H = \sum_\lambda q_\lambda \dot{\Phi}_\lambda - \mathcal{L} = \frac{1}{2}\vec{q}^T[\mathbf{C}^{-1}]\vec{q} + U, \tag{12}
$$

here, $\mathbf{C}^{-1}$ describes the inverse of the capacitance matrix and Cooper-pair number operator is defined as $\hat{n}_\lambda = \hat{q}_\lambda/2e$. The total Hamiltonian of this coupled system can be disclosed as

$$
\hat{H} = 4E_{C_1}\hat{n}_1^2 - E_{J_1}\cos\hat{\phi}_1 + 4E_{C_c}\hat{n}_c^2 - E_{J_c}\cos\hat{\phi}_c + 4E_{C_2}\hat{n}_2^2 - E_{J_2}\cos\hat{\phi}_2 \\
+ 8\frac{C_{1c}}{\sqrt{C_1 C_c}}\sqrt{E_{C_1}E_{C_c}}(\hat{n}_1\hat{n}_c) + 8\frac{C_{2c}}{\sqrt{C_2 C_c}}\sqrt{E_{C_2}E_{C_c}}(\hat{n}_2\hat{n}_c) + 8(1+\eta)\frac{C_{12}}{\sqrt{C_1 C_2}}\sqrt{E_{C_1}E_{C_2}}(\hat{n}_1\hat{n}_2), \tag{13}
$$

where η define as $(C_{1c}C_{2c})/(C_{12}C_c)$. We assumed that the qubit-coupler capacitance is smaller than single-mode capacitance but larger than qubit-qubit coupling capacitance $C_{12} \ll C_{jc} \ll C_\lambda$. In the transmon regime, $E_{J_\lambda}/E_{C_\lambda} \gg 1$, the system Hamiltonian can be expressed as

$$
\hat{H} = \hat{H}_1 + \hat{H}_c + \hat{H}_2 + \hat{H}_{1c} + \hat{H}_{2c} + \hat{H}_{12}, \tag{14}
$$

$$
\hat{H} = \omega_\lambda \hat{b}_\lambda^\dagger \hat{b}_\lambda + \frac{\alpha_\lambda}{2}\hat{b}_\lambda^\dagger \hat{b}_\lambda^\dagger \hat{b}_\lambda \hat{b}_\lambda, \quad \lambda \in \{1, c, 2\}, \tag{15}
$$

$$
\hat{H}_{jc} = g_j(\hat{b}_j^\dagger \hat{b}_c + \hat{b}_j \hat{b}_c^\dagger - \hat{b}_j^\dagger \hat{b}_c^\dagger - \hat{b}_j \hat{b}_c), \quad j = 1, 2, \tag{16}
$$

$$
\hat{H}_{12} = g_{12}(\hat{b}_1^\dagger \hat{b}_2 + \hat{b}_1 \hat{b}_2^\dagger - \hat{b}_1^\dagger \hat{b}_2^\dagger - \hat{b}_1 \hat{b}_2), \tag{17}
$$

where $\hat{b}_\lambda^\dagger$ and $\hat{b}_\lambda$ are the creation and annihilation operators corresponding to each mode. And $\omega_\lambda =$

$\sqrt{8E_{J_\lambda}E_{C_\lambda}} - E_{J_\lambda}$ defines the oscillator frequency, $g_j = \frac{1}{2}\frac{C_{jc}}{\sqrt{C_j C_c}}\sqrt{\omega_j\omega_c}$ and $g_{12} = \frac{1}{2}(1+\eta)\frac{C_{12}}{\sqrt{C_1 C_2}}\sqrt{\omega_1\omega_2}$ expresses qubit-coupler and qubit-qubit coupling strength respectively. In the dispersive regime, where, the coupler frequency is higher than the qubit frequency, the contributions from the double excitation and de-excitation will be significant that's why in Eq. (16) we keep usual Jaynes-Cummings interaction term $(\hat{b}_j^\dagger \hat{b}_c + \hat{b}_j \hat{b}_c^\dagger)$ as well as counter-rotating term $(\hat{b}_j^\dagger \hat{b}_c^\dagger + \hat{b}_j \hat{b}_c)$.

III. MODELING AND SCHRIEFFER-WOLFF TRANSFORMATION

We consider a chain of three modes with exchange coupling between nearest neighbor (NN) and next-nearest neighbors (NNN), as shown in Fig. 1(b). The two qubits (ω_1 and ω_2) coupled to each other with coupling strength g_{12}, as well as each qubit couple to a tunable coupler (ω_c) with coupling strength g_i (i=1,2). Someone can achieve the two level effective Hamiltonian of our our proposed system by changing bosonic operators with Pauli operators as $b^\dagger \rightarrow \sigma^+ (b \rightarrow \sigma^-)$ and $b^\dagger b \rightarrow (|0\rangle\langle 0| - \sigma_z)$. Generally, NN coupling is stronger than NNN coupling, i.e., $g_i > g_{12} > 0$. The Hamiltonian for this two-level system is written as:

$$\hat{H} = \sum_{j=1,2}\frac{1}{2}\omega_j\sigma_j^z + \frac{1}{2}\omega_c\sigma_c^z + \sum_{j=1,2} g_j(\sigma_j^+\sigma_c^- + \sigma_j^-\sigma_c^+) + g_{12}(\sigma_1^+\sigma_2^- + \sigma_1^-\sigma_2^+), \tag{18}$$

where σ_λ^z, σ_λ^+ and σ_λ^- ($\lambda = 1, 2, c$) are Z, raising and lowering Pauli operators, respectively. Here, ω_1 and ω_2 define the frequencies of qubit 1 and 2. These frequencies can be tuned by using energies of capacitors E_{C_λ} and non-linear inductors E_{J_λ}. We define the detuning of two system as $\Delta_j \equiv \omega_j - \omega_c < 0$, here ω_c represents the coupling circuit frequency. In Eq. (18), g_j characterize the coupling strength of qubit with coupler, and g_{12} describes the coupling strength between the qubits. In our proposed model, we use direct coupling and indirect coupling. The indirect coupling is modeled by using qubit, in literature it is called virtual-exchange interaction [26], that can be approximated by the Schrieffer-Wolff transformation (SWT) $U = exp[\sum_{j=1,2}(g_j/\Delta_j)(\sigma_j^+\sigma_c^- - \sigma_j^-\sigma_c^+)]$ [27]. The SWT decouples the coupler from the system, resulting in effective two-qubit Hamiltonian for each mode,

$$\tilde{H} = \sum_{j=1,2}\frac{1}{2}\tilde{\omega}_j\sigma_j^z + \left[\frac{g_1 g_2}{\Delta} + g_{12}\right](\sigma_1^+\sigma_2^- + \sigma_1^-\sigma_2^+), \tag{19}$$

where, $\tilde{\omega}_j = \omega_j + g_j^2/\Delta_j$ defines the Lamb-shifted qubit frequency and the detuning expresses as $1/\Delta = (1/\Delta_1 + 1/\Delta_2) < 0$. Also, we have considered that the coupler qubit stays in its ground state at all times. In Eq. (19), the combined term inside the square brackets represents the total qubit-qubit effective coupling strength $\tilde{g}$, that can be controlled by the coupler frequency through Δ, as well as by using g_1 and g_2, both of which implicitly dependent on ω_c. In general, $\tilde{g}$ is the function of the coupler and qubit frequencies. In the standard two-qubit basis $|00\rangle, |01\rangle, |10\rangle, |11\rangle$, the Hamiltonian of the system can be expressed as

$$\tilde{H} = \begin{pmatrix} \frac{\alpha}{2} & 0 & 0 & 0 \\ 0 & \frac{\tilde{\omega}}{2} & \tilde{g} & 0 \\ 0 & \tilde{g} & -\frac{\tilde{\omega}}{2} & 0 \\ 0 & 0 & 0 & -\frac{\alpha}{2} \end{pmatrix}. \tag{20}$$

The eigenvectors of Hamiltonian in Eq. (20) are given as:

$$|\phi_1\rangle = |0,0\rangle, \qquad |\phi_2\rangle = |1,1\rangle,$$

$$|\phi_3\rangle = \frac{1}{\sqrt{1+\frac{\xi^2}{4\tilde{g}^2}}}\left(\frac{\xi}{2\tilde{g}}|1,0\rangle + |0,1\rangle\right),$$

$$|\phi_4\rangle = \frac{1}{\sqrt{1+\frac{\zeta^2}{4\tilde{g}^2}}}\left(\frac{\zeta}{2\tilde{g}}|1,0\rangle + |0,1\rangle\right), \tag{21}$$

with corresponding eigen energies: $E_1 = -\frac{\alpha}{2}$, $E_2 = \frac{\alpha}{2}$, $E_3 = -\frac{\gamma}{2}$, and $E_4 = \frac{\gamma}{2}$, where $\alpha = \tilde{\omega}_1 + \tilde{\omega}_2$, $\tilde{\omega} = \tilde{\omega}_1 - \tilde{\omega}_2$, $\gamma = \sqrt{4\tilde{g}^2 + \tilde{\omega}^2}$, $\xi = -\tilde{\omega} + \gamma$ and $\zeta = -(\tilde{\omega} + \gamma)$. Note that when $\tilde{\omega} \rightarrow 0$ and $\tilde{g} > 0$, the two states go to the maximally entangled states as $|\phi_3\rangle = \frac{1}{\sqrt{2}}(|01\rangle + |10\rangle)$ and $|\phi_4\rangle = \frac{1}{\sqrt{2}}(|01\rangle - |10\rangle)$. For $\tilde{g} < 0$, both states are converted to $|\phi_3\rangle = \frac{1}{\sqrt{2}}(|01\rangle - |10\rangle)$ and $|\phi_4\rangle = \frac{1}{\sqrt{2}}(|01\rangle + |10\rangle)$. Moreover, we can find that the eigen
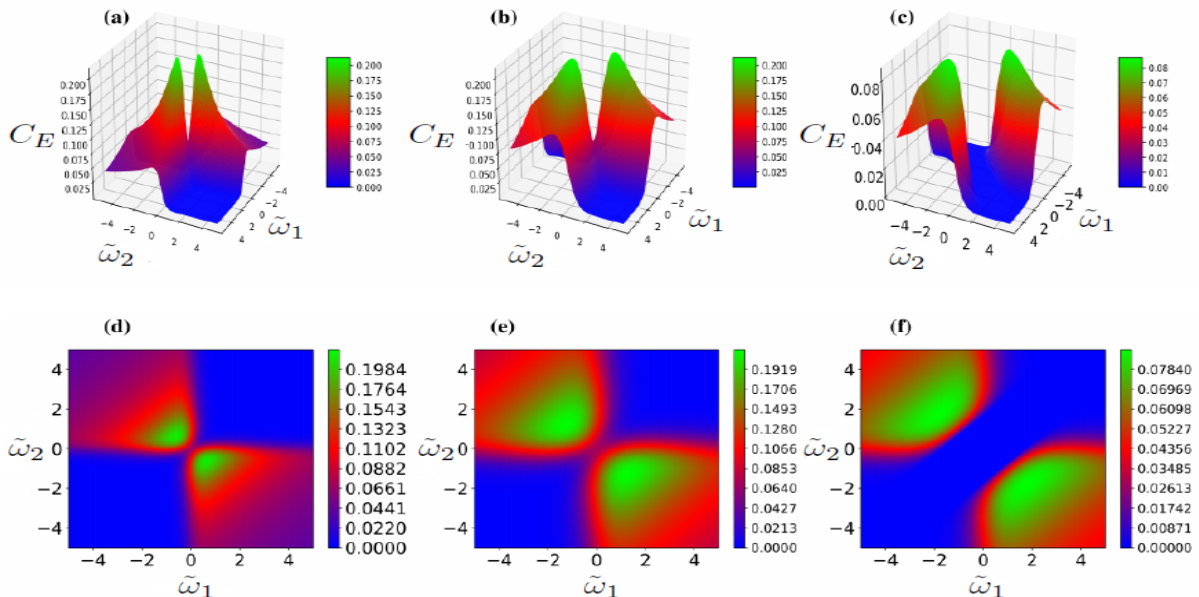
FIG. 3: The two-dimensional concurrence in two coupled qubit system is plotted versus dimensionless frequencies $\tilde{\omega}_1$ and $\tilde{\omega}_2$ for (a,d) $\tilde{g} = T = 0.4$, (b,e) $\tilde{g} = T = 0.2$ and (c,f) $\tilde{g} = 0.2$ & $T = 0.4$. T is plotted in units of Boltzmann's constant where $k_B = 1$.
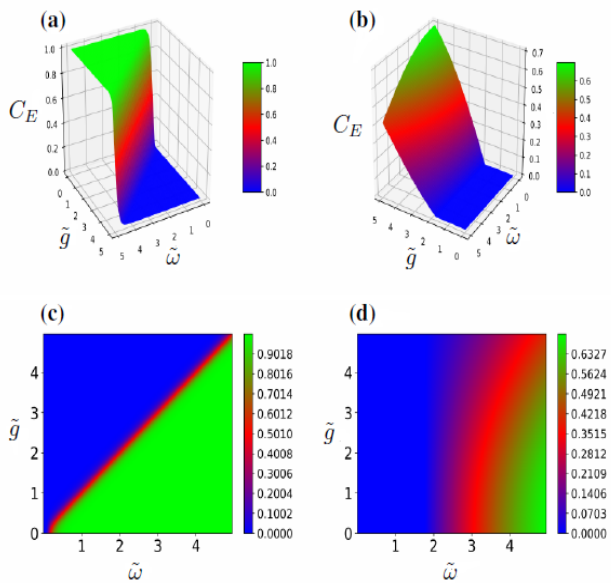

FIG. 4: The two-dimensional concurrence in two coupled qubit system is plotted versus $\tilde{g}$ and $\tilde{\omega}$ for different values of dimensionless temperature (a,c) $T = 0.1$ and for (b,d) $T = 2$.

energies are even function of the effective qubit-qubit coupling $\tilde{g}$. Therefore, the ground-state entanglement exists for both positive direct coupling and negative indirect coupling and it should be symmetric with respect to the effective qubit-qubit coupling $\tilde{g}$. The ground state entanglement depends on the effective qubit-qubit coupling constant $\tilde{g}$, α and γ, as predicted in Eq. (21).

A. Thermal Entanglement

In this subsection, we highlight how quantum entanglement depends on external temperature by making use of the concurrence. The thermal density matrix $\rho(T)$ for this system in terms of standard basis can be written as

$$\rho(T) = \frac{e^{-\beta H}}{Z} = \frac{1}{Z} \sum_{i=1}^{4} e^{-\beta E_m} |\psi_i\rangle \langle\psi_i|, \qquad (22)$$

$$\rho(T) = \frac{1}{Z} \begin{pmatrix} \rho_{11} & 0 & 0 & 0 \\ 0 & \rho_{22} & \rho_{23} & 0 \\ 0 & \rho_{32} & \rho_{33} & 0 \\ 0 & 0 & 0 & \rho_{44} \end{pmatrix}, \qquad (23)$$

where $\beta = 1/(k_B T)$, $\rho_{11} = e^{-\alpha/2T}$, $\rho_{22} = \rho_{33} = \frac{\gamma^2 \cosh\left(\frac{\gamma}{2T}\right) + \gamma\tilde{\omega}\sinh\left(\frac{\gamma}{2T}\right)}{\gamma^2}$, $\rho_{23} = \rho_{32} = \frac{2\tilde{g}\sinh\left(\frac{\gamma}{2T}\right)}{\gamma}$ and $\rho_{44} = e^{\alpha/2T}$. For convenience, we choose $k_B = 1$ throughout these calculations. However, someone can get SI units of temperature by using this relation $T' = \frac{\hbar\omega}{k_B T}$, here $\omega \sim 4$ GHz and T' is defined in mK. The partition function Z is calculated as

$$Z = 2\left[\cosh\left(\frac{\alpha}{2T}\right) + \cosh\left(\frac{\gamma}{2T}\right)\right]. \qquad (24)$$

The concurrence 0 corresponds to separable or unentangled states and 1 defines maximally entangled states and is expressed as [28],

$$C_E = max\left[0, \lambda_1 - \lambda_2 - \lambda_3 - \lambda_4\right], \qquad (25)$$

where, λ_i's are the square root of the eigenvalues of the matrix R, which we can calculate with the help of Eq. (23). To observe the effect of coupling strength, temperature, and qubit frequencies on the quantum entanglement, we divide our discussion into three special cases.

Case 1: In the first scenario, we would like to discuss the dependence of quantum entanglement on the coupling strength $\tilde{g}$ and on the temperature T as shown in Fig. 2. In this special case, we let the qubit frequencies are constant. We let $\tilde{\omega}_1 = \tilde{\omega}_2 = 1$, we notice that the two qubits are maximally entangled for $\tilde{g} = 5$ and for $T \to 0$. However, as the temperature started to increase the concurrence is started to become zero. It means that the two qubits are less entangled for high temperature, as shown in Fig. 2(a). On the other hand, if $\tilde{\omega}_1 \neq \tilde{\omega}_2$, the entanglement gets vanishes for low temperature too, even though the coupling strength is quite high as shown in Fig. 2(b). Additionally, for higher coupling strength, the entanglement strength is quite weak as compared to the first scenario, when qubit frequencies are equal. Therefore, our results suggest that for strong entanglement it is better to have superconducting qubits with the same frequencies.

Case 2: To see the effect of superconducting qubit frequency on the quantum entanglement for constant temperature and coupling strength, we plot Fig. 3. The values of the frequencies can be tuned by using E_J and E_C. We can achieve the negative regime of the frequency by letting $\frac{E_J}{E_C} < \frac{1}{8}$. We notice that the quantum entanglement vanishes when both frequencies become zero, which is indeed true as there is no qubit left for the entanglement. We also observe that for small values of equal frequencies, the chances of qubits entanglement are high as compare to high frequencies. On the other hand, if the two-qubit frequencies are different from each other, then there are very less chances that qubits get entanglement. If one qubit frequency is negative and the other is positive then we find high chances to get quantum entanglement as shown in Fig. 3(b), for $\tilde{g} = T = 0.2$. For coupling strength $\tilde{g} = 0.2$ and temperature $T = 0.4$, we notice that the entanglement is only possible for high-frequency superconducting qubits. In another way, we can say that it is less probable that the two qubits get entangled for lower frequencies, high temperature, and low coupling strength.

Case 3: In this special case, we calculate quantum entanglement dependence on the coupling strength and frequencies of the qubits, for a constant temperature. We note that for $T = 0.1$, the concurrence is 1 for small values of coupling strength and for high values of frequencies as shown in Fig. 4(a) and 4(c). However, as we increase the frequency the concurrence goes to zero for low coupling strength, as shown in 4(c). However, as we increase the temperature $T = 2$, the transition from entangle states to unentangle states happen near $\tilde{\omega} \leq 2$. This graph shows that the entangled states are possible for higher frequencies and low coupling strength.

IV. CONCLUSION

In conclusion, by using the concept of concurrence we have investigated the thermal entanglement in two coupled superconducting qubits under the influence of arbitrary coupling strength. Our proposed model is quite realistic, therefore, it can be experimentally implemented and all the parameters are tunable. We have found that the thermal entanglement can be efficiently controlled through the effective qubit-qubit coupling strength, qubit frequencies, and temperature. The effects of affective qubit-qubit coupling strength and temperature on entanglement are studied for different values of qubit frequencies. We find that entanglement exists and it can be enhanced by using the coupled qubits with the same frequencies. Our results imply that the two coupled qubits can go to maximally entangled states at low temperature and for equal and high values of qubit frequencies. Our proposed model can further be enhanced for gates, where, someone can study the effect of temperature on the fidelity of quantum gates. This model can also be beneficial for study thermal entanglement for many $(n > 2)$ qubit states. Our findings identify the real potential to study thermal entanglement, especially for superconducting qubits.

V. ACKNOWLEDGMENT

References

---

* Electronic address: javedakram@daad-alumni.de

[1] D. Ventura and S. Kak, Information Sciences **128**, 147 (2000), ISSN 0020-0255, URL http://doi.org/10.1016/s0020-0255%2800%2900049-9.

[2] J. Akram and F. Saif, Journal of Russian Laser Research **29**, 538 (2008), ISSN 1071-2836,1573-8760, URL http://doi.org/10.1007/s10946-008-9045-y.

[3] T. D. Ladd, F. Jelezko, R. Laflamme, Y. Nakamura, C. Monroe, and J. L. O'Brien, Nature **464**, 45 (2010), ISSN 0028-0836,1476-4679, URL http://doi.org/10.1038/nature08812.

[4] J. Kelly, R. Barends, A. G. Fowler, A. Megrant, T. C. Jeffrey, E.; White, D. Sank, J. Y. Mutus, B. Campbell, Y. Chen, Z. Chen, et al., Nature **519**, 66 (2015),

ISSN 0028-0836,1476-4679, URL http://doi.org/10.1038/nature14270.

[5] C. Song, K. Xu, W. Liu, C.-p. Yang, S.-B. Zheng, H. Deng, Q. Xie, K. Huang, Q. Guo, L. Zhang, et al., Phys. Rev. Lett. **119**, 180511 (2017), URL https://link.aps.org/doi/10.1103/PhysRevLett.119.180511.

[6] H. Bernien, S. Schwartz, A. Keesling, H. Levine, A. Omran, H. Pichler, S. Choi, M. Zibrov, Alexander S.and Endres, M. Greiner, V. Vuletić, et al., Nature **551**, 579 (2017), ISSN 0028-0836,1476-4679, URL http://doi.org/10.1038/nature24622.

[7] J. Zhang, G. Pagano, P. W. Hess, A. Kyprianidis, P. Becker, H. Kaplan, A. V. Gorshkov, Z.-X. Gong, and C. Monroe, Nature **551**, 601 (2017), ISSN 0028-0836,1476-4679, URL http://doi.org/10.1038/nature24654.

[8] K. J. Sung, J. Yao, M. P. Harrigan, N. C. Rubin, Z. Jiang, L. Lin, R. Babbush, and J. R. McClean, Quantum Science and Technology **5**, 044008 (2020), URL https://doi.org/10.1088/2058-9565/abb6d9.

[9] L. Xiang-Ping, F. Mao-Fa, Z. Xiao-Juan, and C. Jian-Wu, Chinese Physics Letters **23**, 3138 (2006), URL https://doi.org/10.1088/0256-307x/23/12/004.

[10] J. Q. You, X. Hu, S. Ashhab, and F. Nori, Phys. Rev. B **75**, 140515 (2007), URL https://link.aps.org/doi/10.1103/PhysRevB.75.140515.

[11] M. Steffen, S. Kumar, D. P. DiVincenzo, J. R. Rozen, G. A. Keefe, M. B. Rothwell, and M. B. Ketchen, Phys. Rev. Lett. **105**, 100502 (2010), URL https://link.aps.org/doi/10.1103/PhysRevLett.105.100502.

[12] F. Yan, S. Gustavsson, A. Kamal, J. Birenbaum, A. P. Sears, D. Hover, T. J. Gudmundsen, D. Rosenberg, G. Samach, S. Weber, et al., Nature Communications **7**, 12964 (2016), ISSN 2041-1723, URL http://doi.org/10.1038/ncomms12964.

[13] J. Koch, T. M. Yu, J. Gambetta, A. A. Houck, D. I. Schuster, J. Majer, A. Blais, M. H. Devoret, S. M. Girvin, and R. J. Schoelkopf, Phys. Rev. A **76**, 042319 (2007), URL https://link.aps.org/doi/10.1103/PhysRevA.76.042319.

[14] R. Barends, J. Kelly, A. Megrant, D. Sank, E. Jeffrey, Y. Chen, Y. Yin, B. Chiaro, J. Mutus, C. Neill, et al., Phys. Rev. Lett. **111**, 080502 (2013), URL https://link.aps.org/doi/10.1103/PhysRevLett.111.080502.

[15] J.-H. An, S.-J. Wang, and H.-G. Luo, Physica A: Statistical Mechanics and its Applications **382**, 753 (2007), ISSN 0378-4371, URL http://doi.org/10.1016/j.physa.2007.04.008.

[16] A. Erika and O. Patrik, Quantum Information and Coherence, Scottish Graduate Series (Springer International Publishing, 2014), 1st ed., ISBN 978-3-319-04062-2,978-3-319-04063-9, URL http://gen.lib.rus.ec/book/index.php?md5=c947b851a9449a86b09c2f533d2340df.

[17] D. Chruscinski and A. Rutkowski, The European Physical Journal D / Atomic, Molecular, Optical and Plasma Physics **62**, 273 (2011), ISSN 1434-6060,1434-6079, URL http://doi.org/10.1140/epjd%2Fe2011-10450-8.

[18] G.-F. Zhang and S.-S. Li, Phys. Rev. A **72**, 034302 (2005), URL https://link.aps.org/doi/10.1103/PhysRevA.72.034302.

[19] W. K. Wootters, Phys. Rev. Lett. **80**, 2245 (1998), URL https://link.aps.org/doi/10.1103/PhysRevLett.80.2245.

[20] M. C. Arnesen, S. Bose, and V. Vedral, Phys. Rev. Lett. **87**, 017901 (2001), URL https://link.aps.org/doi/10.1103/PhysRevLett.87.017901.

[21] A. Blais, A. M. van den Brink, and A. M. Zagoskin, Phys. Rev. Lett. **90**, 127901 (2003), URL https://link.aps.org/doi/10.1103/PhysRevLett.90.127901.

[22] S. Hill and W. K. Wootters, Phys. Rev. Lett. **78**, 5022 (1997), URL https://link.aps.org/doi/10.1103/PhysRevLett.78.5022.

[23] J. Q. You and F. Nori, Nature **474**, 589 (2011), ISSN 0028-0836,1476-4679, URL http://doi.org/10.1038/nature10122.

[24] G. Wendin and V. S. Shumeiko, Low Temperature Physics **33**, 724 (2007), ISSN 1063-777X,1090-6517, URL http://doi.org/10.1063/1.2780165.

[25] F. Yan, P. Krantz, Y. Sung, M. Kjaergaard, D. L. Campbell, T. P. Orlando, S. Gustavsson, and W. D. Oliver, Phys. Rev. Applied **10**, 054062 (2018), URL https://link.aps.org/doi/10.1103/PhysRevApplied.10.054062.

[26] A. Blais, J. Gambetta, A. Wallraff, D. I. Schuster, S. M. Girvin, M. H. Devoret, and R. J. Schoelkopf, Phys. Rev. A **75**, 032329 (2007), URL https://link.aps.org/doi/10.1103/PhysRevA.75.032329.

[27] S. Bravyi and D. P. D. D. Loss, Annals of Physics **326**, 2793 (2011), ISSN 0003-4916,1096-035X, URL http://doi.org/10.1016/j.aop.2011.06.004.

[28] P. Rungta and C. M. Caves, Phys. Rev. A **67**, 012307 (2003), URL https://link.aps.org/doi/10.1103/PhysRevA.67.012307.